AGU PUBLICATIONS

Geophysical Research Letters

RESEARCH LETTER
10.1002/2017GL074557

Key Points:
- The timing and magnitude of events largely depend on the phase of discharges
- Events are not substantially affected by the timing of a sudden recharge
- Simulations are used to analyze the unexpected behavior of recent EN events

Supporting Information:
- Supporting Information S1

Correspondence to:
J. Ballester,
joan.ballester@isglobal.org

Citation:
Ballester, J., D. Petrova, S. Bordoni, B. Cash, and X. Rodó (2017), Timing of subsurface heat magnitude for the growth of El Niño events, *Geophys. Res. Lett.*, *44*, 8501–8509, doi:10.1002/2017GL074557.

Received 14 JUN 2017
Accepted 30 JUL 2017
Accepted article online 3 AUG 2017
Published online 19 AUG 2017

Timing of subsurface heat magnitude for the growth of El Niño events

Joan Ballester[1,2,3], Desislava Petrova[1,3], Simona Bordoni[2], Ben Cash[4], and Xavier Rodó[1,3,5]

[1]Climate and Health Program, Barcelona Institute for Global Health (ISGlobal), Barcelona, Spain, [2]California Institute of Technology (Caltech), Pasadena, California, USA, [3]Institut Català de Ciències del Clima (IC3), Barcelona, Spain, [4]Center for Ocean–Land–Atmosphere Studies, George Mason University, Fairfax, Virginia, USA, [5]Institució Catalana de Recerca i Estudis Avançats, Barcelona, Spain

Abstract The subsurface heat buildup in the western tropical Pacific and the recharge phase in equatorial heat content are intrinsic elements of El Niño–Southern Oscillation, leading to changes in zonal wind stress, sea surface temperature, and thermocline tilt that characterize the growing and mature phases of El Niño (EN) events. Here we use numerical simulations to study the impact on subsequent EN episodes of a sudden increase or decrease in ocean heat content during the recharge phase and compare results with previous studies in which this perturbation is prescribed earlier during the tilting mode. We found that while not substantially affected by the phase at which a sudden rise in heat content is prescribed, the timing and magnitude of the events are very sensitive to the phase at which a major decrease is imposed. The different response to the phase of increases and decreases substantiates the importance of nonlinear subsurface ocean dynamics to the onset and growth of EN episodes and provides insight into the irreversibility of the events at different stages of the oscillation.

1. Introduction

El Niño–Southern Oscillation (ENSO) is the dominant variability mode at interannual timescales [*Wang and Picaut*, 2004], a primary source of seasonal-to-interannual climate predictability [*Chen et al.*, 2004; *Izumo et al.*, 2010; *Barnston et al.*, 2012; *Petrova et al.*, 2016], and a key factor explaining large-scale teleconnections [*Ballester et al.*, 2011] with global impacts [*Ballester et al.*, 2013, 2016a]. The dynamics of ENSO arise from a complex interaction between the atmosphere and the ocean in the tropical Pacific [*Bjerknes*, 1969; *McPhaden et al.*, 2006], involving upper and lower level atmospheric winds, ocean waves traveling along the equatorial thermocline, zonal redistribution of surface and subsurface ocean temperatures, and meridional recharge or discharge of the tropical ocean heat content [*Suarez and Schopf*, 1988; *Jin*, 1997; *Picaut et al.*, 1997; *Weisberg and Wang*, 1997; *Fedorov et al.*, 2015].

ENSO is typically characterized by its two main opposite phases, El Niño (EN) and La Niña (LN), which define an anomalous warming or cooling of sea surface temperatures (SSTs) in the central and eastern tropical Pacific, respectively. EN (LN) is always preceded by a meridional recharge (discharge) of basin-wide tropical ocean heat content about two to three seasons in advance, which deepens (shoals) the whole equatorial thermocline and warms (cools) the ocean subsurface at about 100 to 150 m depth [*Meinen and McPhaden*, 2000; *Ramesh and Murtugudde*, 2013]. This phase is in turn typically led by the tilting mode, a maximum (minimum) in the slope of the equatorial thermocline explained by the strengthening (weakening) of the equatorial trade winds and the subsequent anomalous downwelling (upwelling) of surface warm (subsurface cold) waters in the western Pacific warm pool [*Wyrtki*, 1985; *Ballester et al.*, 2015].

The leading paradigm explaining the oscillatory nature of ENSO, the recharge oscillator, emphasizes the delayed effect of the enhancement (weakening) of the equatorial trade winds that precedes the recharge (discharge) phase. Thus, the off-equatorial wind stress curl controls the change rate in equatorward subsurface convergence (divergence) of water masses in the central Pacific, and therefore the tendency toward the deepening (shoaling) of the thermocline [*Jin*, 1997]. Once the equatorial trade winds return to their climatological values, westerly (easterly) wind bursts can occur and trigger eastward traveling downwelling (upwelling) Kelvin waves that deepen (shoal) the thermocline in the eastern Pacific, suppress (enhance) the coastal upwelling there, and activate the growth of an EN (LN) event [*Ballester et al.*, 2016b]. This succession of phases is, however, subject to sources of irregularity, so that it is nowadays widely accepted that ENSO is a slightly damped periodic oscillation modulated by stochastic noise [*Kessler*, 2002].

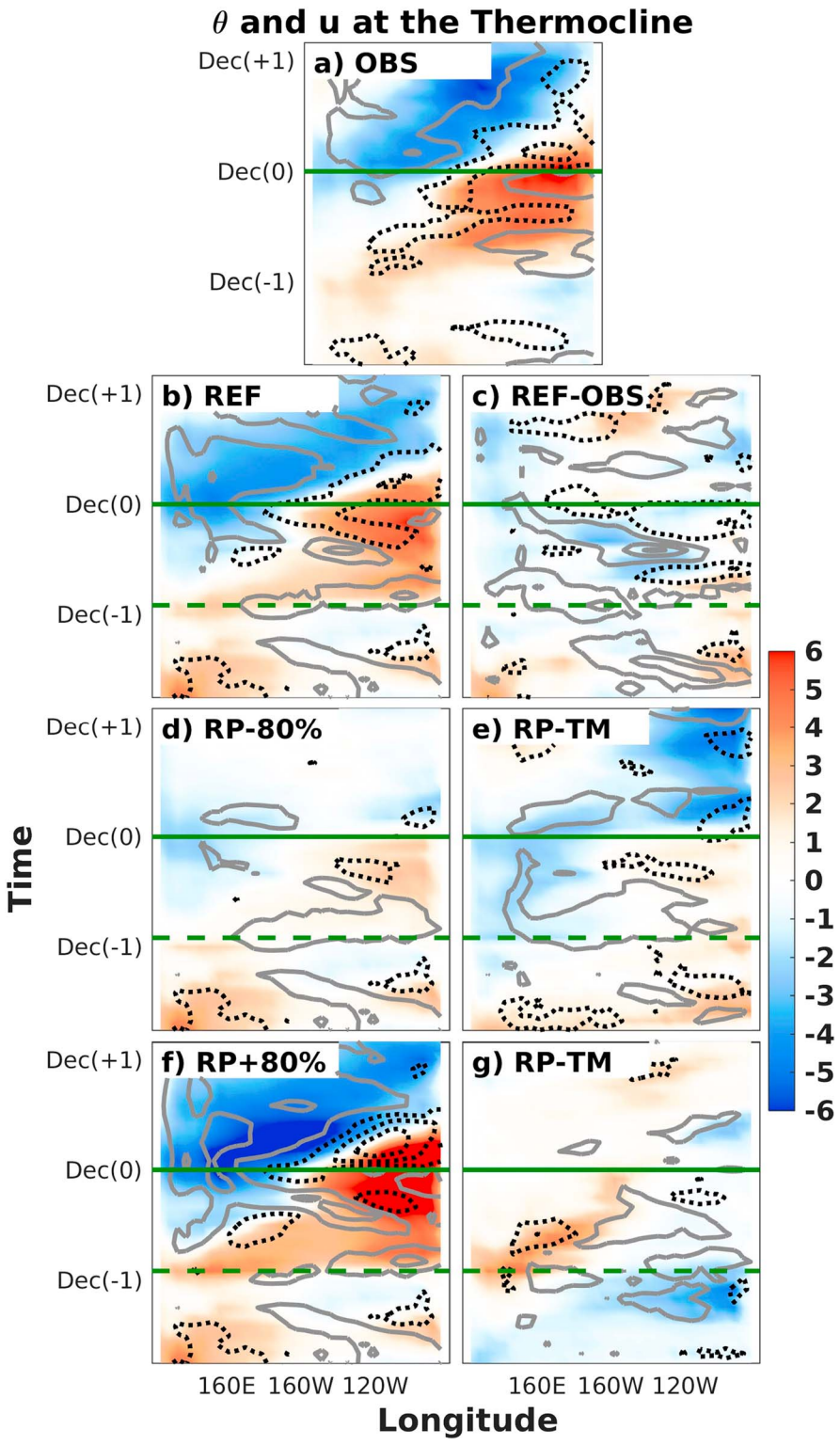

Figure 1. Longitude-time Hovmöller diagram of equatorial temperature (shading, in °C) and zonal current (contour, in m/s) anomalies at the level of the thermocline. Panels correspond to the observation composite of the December 1972, 1982, and 1997 (a) El Niño events, the (b) reference simulation, and an 80% (d) reduction or (f) amplification of the subsurface warming during the recharge phase. The other panels show the differences (c) between the reference simulation and the observations and (e and g) between the recharge phase and tilting mode experiments. The minimum contour is ±0.1 m/s, and the contour interval is 0.2 m/s, with grey solid (black dashed) lines depicting positive (negative) anomalies. The solid (dashed) green lines indicate the peak of El Niño (the recharge phase) in the reference simulation.

Ballester et al. [2016c] recently studied the sensitivity of EN to a rise or fall in ocean heat content 21 months earlier by means of an ensemble of numerical simulations. These experiments showed that basin-wide uniform warm equatorial SSTs follow a major increase in heat content, which favor the occurrence of a very strong EN event 1 year later. The simulations also showed that the heat content of the system is naturally restored after an initial major decrease; the resulting EN event is, however, delayed by up to 1 year. In the present study, we extend this analysis with a new set of numerical experiments, in which we use exactly the same methodology, but initial conditions are modified at a later stage of the onset of EN. More specifically, we compare these two families of simulations with the aim of identifying the dynamical mechanisms that explain how differences in the lead time of a sudden rise or fall in heat content affect subsequent EN events.

2. Methods

The model used here is the Community Earth System Model (CESM) v1.2 [*Hurrell et al.*, 2013]. The atmospheric component has a resolution of 2.5° in longitude and 1.875° in latitude, with 30 vertical levels. The ocean model uses a displaced pole grid with approximately 1° resolution in longitude and 0.5° in latitude, which is refined within the tropical band up to 0.25° at the equator. There are 60 vertical levels, with vertical resolution decreasing from 10 m in the upper 150 m to 250 m in the deep ocean.

An EN episode with the same magnitude as the recent 2015/2016 event (i.e., Niño3.4 Index = +2.8°C) was chosen from a reference (REF) 100 year spin-up simulation, which is validated against the composite of the 1972/1973 (+2.5°C), 1982/1983 (+2.6°C), and 1997/1998 (+2.7°C) EN events in the ORAS4 [*Balmaseda et al.*, 2013] and National Centers for Environmental Prediction/National Center for Atmospheric Research [*Kalnay et al.*, 1996] reanalyses (here referred to as observational composite, and labeled as OBS).

We describe a new family of ensemble experiments with initial conditions corresponding to a lead time of 11 months before the December peak of this event (i.e., 1 January of year 0) and compare the results with a family initialized 10 months earlier (i.e., 1 March of year −1, simulations reported in *Ballester et al*. [2016c]). We note that these stages of the episode correspond to an early phase of the basin-wide deepening of the thermocline (referred here to as RP, standing for Recharge Phase) and the maximum in the slope of the equatorial thermocline (TM for Tilting Mode), respectively.

In each of these families, the intensity of the initial subsurface warm anomaly was decreased (negative sign) or increased (positive sign). The warm temperature anomalies were fully modified only in the inner three-dimensional box [120°E–80°W] × [10°S–10°N] × [50–200 m], and this modification was linearly decreased to zero from the border of this inner box to the frontier of the outer box [100°E–60°W] × [15°S–15°N] × [20–300 m]. Each set of experiments in turn consists of 10 simulations with slightly perturbed initial conditions.

3. Results

The comparison with the observation composites (Figures 1a, 2a, and 3a) shows that the REF simulation correctly reproduces the main dynamical processes preceding the peak of the observed major EN events and the subsequent transition toward LN, including the main subsurface ocean features and the coupling between the ocean surface and the atmosphere (Figures 1b, 2b, and 3b). The model, for example, simulates the slow but steady pileup of subsurface warm waters in the western Pacific near and above the thermocline, due to stronger-than-normal easterly trade winds in the central Pacific during year −1, and the associated downward heat advection in the warm pool (Figures 1c, 2c, and 3c). Some differences are, however, found, e.g., the westerly wind anomalies are stronger in the model than in the observation composites during the growing and decaying phases of EN, which in turn explains the warm SST bias in the central Pacific (Figure 2c). The differences between the observational composites and the REF simulation are, however, relatively small for the type of dynamical processes and empirical relationships that are the focus of the present work, which are to a large extent associated with the onset of the EN episodes in the ocean subsurface several months before their mature phase.

The transition from the initial tilting mode to the recharge phase (i.e., the two stages that are here compared) is seen to be associated with anomalies in the wind stress curl, which, according to the recharge theory,

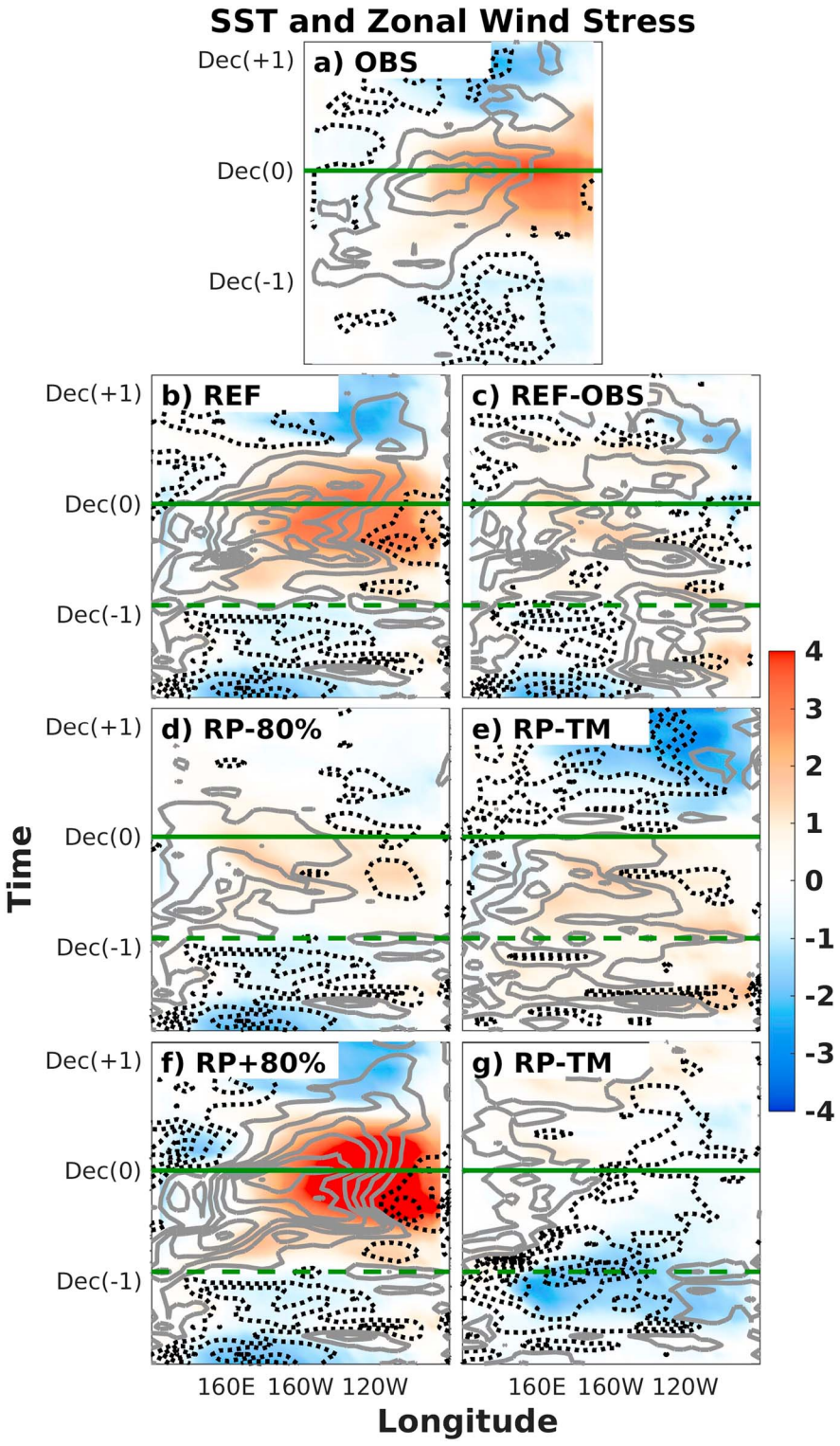

Figure 2. Longitude-time Hovmöller diagram of sea surface temperature (shading, in °C) and surface zonal wind (contour, in m/s) anomalies. Panels correspond to the observation composite of the December 1972, 1982, and 1997 (a) El Niño events, the (b) reference simulation, and an 80% (d) reduction or (f) amplification of the subsurface warming during the recharge phase. The other panels show the differences (c) between the reference simulation and the observations and (e and g) between the recharge phase and tilting mode experiments. The minimum contour is ±0.5 m/s, and the contour interval is 1 m/s, with grey solid (black dashed) lines depicting positive (negative) anomalies. The solid (dashed) green lines indicate the peak of El Niño (the recharge phase) in the reference simulation.

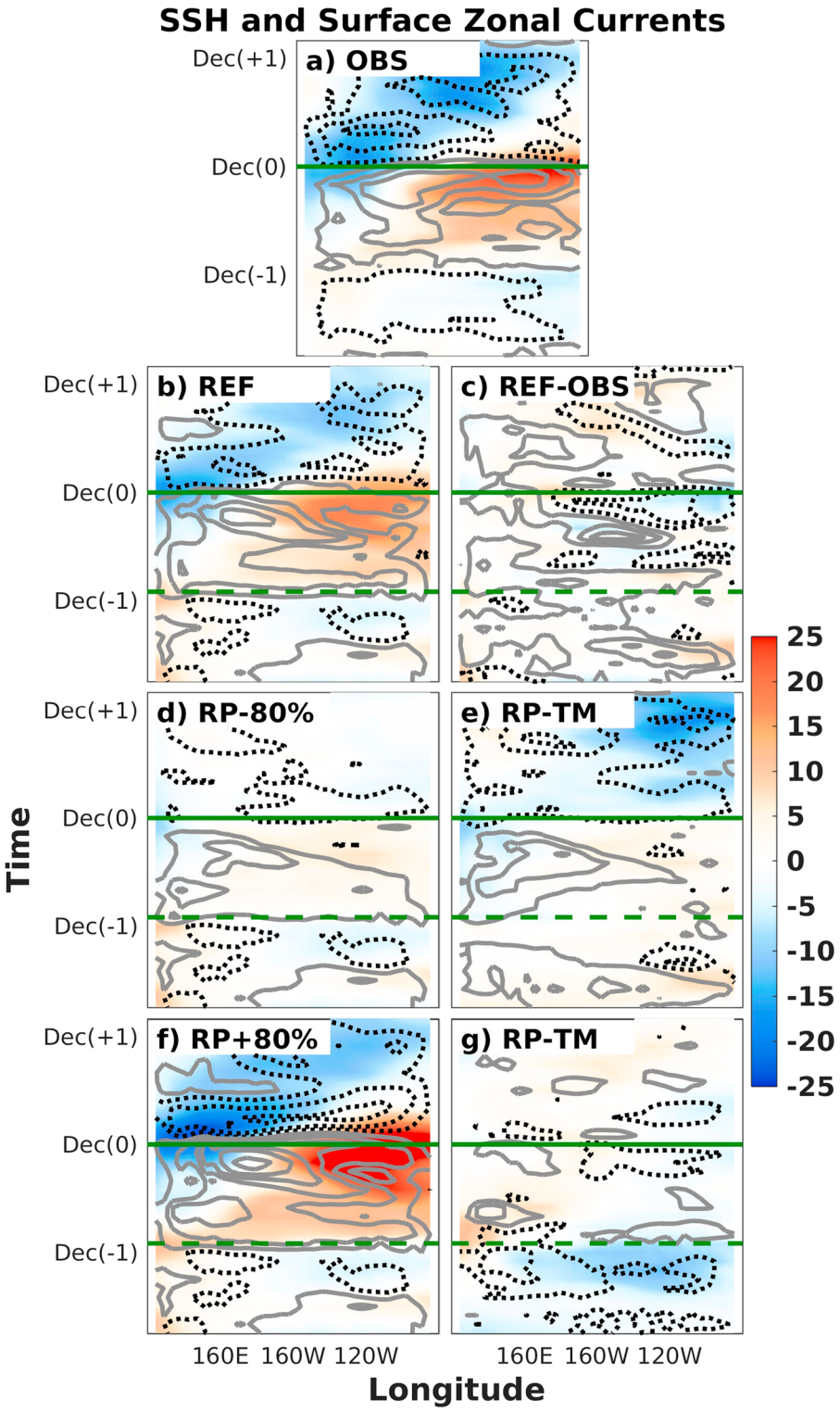

Figure 3. Longitude-time Hovmöller diagram of sea surface height (shading, in cm) and surface zonal current (contour, in m/s) anomalies. Panels correspond to the observation composite of the December 1972, 1982, and 1997 (a) El Niño events, the (b) reference simulation, and an 80% (d) reduction or (f) amplification of the subsurface warming during the recharge phase. The other panels show the differences (c) between the reference simulation and the observations and (e and g) between the recharge phase and tilting mode experiments. The minimum contour is ±0.1 m/s, and the contour interval is 0.2 m/s, with grey solid (black dashed) lines depicting positive (negative) anomalies. The solid (dashed) green lines indicate the peak of El Niño (the recharge phase) in the reference simulation.

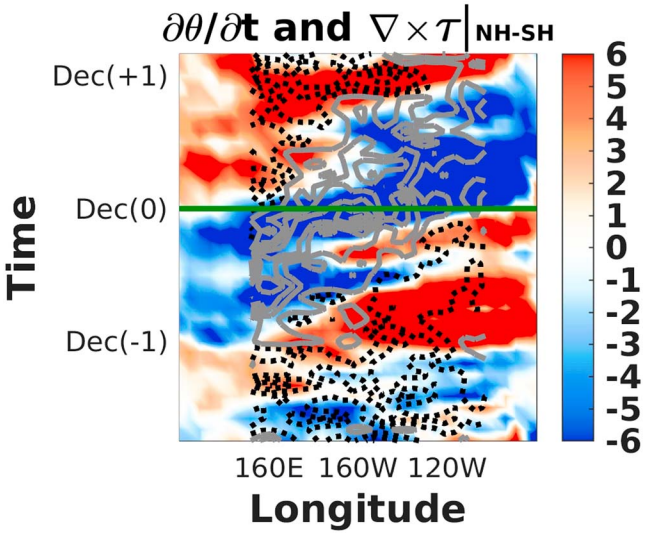

Figure 4. Longitude-time Hovmöller diagram of anomalies in equatorial temperature tendency at the level of the thermocline (shading, in °C/yr) and the interhemispheric difference in wind stress curl between [0,20°N] and [20°S,0] (contour, in N/m^3). The panel corresponds to the observation composite of the December 1972, 1982, and 1997 El Niño events. The minimum contour is $\pm 0.5 \cdot 10^{-8}$ N/m^3, and the contour interval is 10^{-8} N/m^3, with grey solid (black dashed) lines depicting positive (negative) anomalies. The solid green line indicates the peak of El Niño.

generates equatorward subsurface convergence of water masses in the central Pacific, and therefore the tendency toward the overall deepening of the thermocline [*Jin*, 1997]. Figure 4 shows that the interhemispheric difference (Northern Hemisphere minus Southern Hemisphere) of the tropical wind stress curl is negative throughout year −1 in the whole basin, as well as in the central and eastern Pacific during the stages of largest warming rate in year 0. *Ballester et al.* [2016b] showed that a fraction of this subsurface warming is additionally explained by zonal and vertical advection of heat along the subsurface currents near the tilted thermocline. We note that positive anomalies in interhemispheric wind stress curl difference also coincide with the eastward propagating subsurface cooling tendency and the associated transition towards LN conditions in year +1 [*McGregor et al.*, 2012].

In agreement with the observational composites, the initial conditions in the RP experiments were prescribed at the beginning of the last month in which the ocean surface and the atmosphere are in a neutral phase in the REF simulation (e.g., last month with slightly negative values of the Niño3.4 Index; Figure S1b in the supporting information). Just a few months later, in early spring of year 0, the first strong westerly wind anomalies develop in the warm pool (dashed green line in Figure 2b): as a result, the downwelling Kelvin waves start to cross the basin (Figure 3b) and the accumulated subsurface heat reaches the eastern Pacific (Figure 1b). The timely prescription of subsurface heat content anomalies in the RP experiment just before the activation of the Bjerknes feedback is therefore designed to provide some insight into the irreversibility of the EN event at this advanced stage of the oscillation.

A sudden reduction of 80% in the heat content stored in the ocean subsurface during the recharge phase (i.e., experiment RP-80%) does not significantly modify the dynamical mechanisms that precede the peak of the episode in the REF simulation (Figures 1d, 2d, 3d, and S1). As a result, the timing of the subsequent EN event remains essentially unaffected, and the anomaly of the Niño3.4 Index reaches +1.15°C, which represents a nearly proportional relative decrease of about 60%. The maximum in westerly wind and SST anomalies is, however, found to occur earlier, in August of year 0, so that the heat content in the basin is completely discharged by the end of the year and the Niño3.4 Index returns to values close to 0 in March of year +1. The fast and early termination of the event generates very weak cold subsurface temperature anomalies and no reinforcement of the trade winds in the warm pool, which explains the lack of a LN event by the end of year +1.

The dynamics of ENSO in the RP-80% experiment are completely different from those resulting from the ensemble of simulations in which the same fraction of the heat content is removed during the tilting mode 10 months earlier (i.e., TM-80%). *Ballester et al.* [2016c] showed that in these runs a weak LN event develops at the end of year −1, which reactivates the generation of the subsurface heat buildup in the western Pacific and leads to a strong EN episode that peaks in December of year +1 (Niño3.4 Index = +2°C). Differences between both cases therefore highlight the importance of the timing of the prescribed decrease in heat content (Figures 1e, 2e, and 3e). When this reduction occurs during the tilting mode, the system is forced to take a step back and restore the heat content; if the decrease occurs just before the maximum of the recharge

phase, the system is at a point of no return in which the remaining heat is immediately released to the eastern Pacific, leading to a weak EN event. Differences in the timing of the initial reduction in heat content and the eventual occurrence of a restoring process have a substantial effect on the magnitude of the subsequent EN event, with the event occurring with 1 year of delay in TM-80% and being almost twice as large than the one in RP-80%.

The response of the coupled ocean-atmosphere system to a sudden amplification of 80% in the heat content during the recharge phase (i.e., experiment RP + 80%) is immediate, with the excess heat being released as eastward traveling downwelling Kelvin waves and leading to an event of very strong magnitude at the end of the year (Niño3.4 Index = +4°C; Figures 1f, 2f, 3f, and S1). A similar immediate release of the excess heat was described in *Ballester et al*. [2016c] for the TM + 80% experiment 10 months earlier, but in that case, the surface warming at the end of year −1 was found to be uniformly distributed along the equatorial Pacific. Under these conditions, the Bjerknes feedback cannot be activated, and therefore, the initial warming only represents a transition step toward a very strong EN episode of similar magnitude 1 year later. For this reason, even if there are important differences in the involved dynamical mechanisms, anomalies in atmospheric winds, heat content and surface, and subsurface temperatures and currents are relatively similar between the two experiments (Figures 1g, 2g, and 3g).

4. Discussion and Summary

Previous studies have argued that there exists a boreal winter barrier in equatorial Pacific upper ocean heat content predictability due to a seasonal minimum in overall variability [*Balmaseda et al*., 1995; *McPhaden*, 2003], in addition to the well-known boreal spring barrier in atmosphere and surface ocean ENSO predictability. As a result of this boreal winter barrier, equatorial Pacific upper ocean heat content anomalies in boreal autumn and early winter (i.e., September to January) do not necessarily persist until the following winter season, while anomalies that exist in late boreal winter and spring (i.e., February to May) tend to persist for the next two to three seasons [*McPhaden*, 2003]. Because of this, equatorial heat content anomalies in boreal autumn and early winter are not necessarily associated with ENSO events the following year. We have here chosen January of year 0 as a particularly relevant time of the year to prescribe a sudden change in heat content, in order to test the inertia of the oscillation to perturbations in the evolution of subsurface temperatures. On the one hand, it follows the boreal winter barrier in equatorial Pacific upper ocean heat content predictability, whose role can be evaluated through the analysis of the differences between the TM and RP experiments. On the other hand, it precedes the boreal spring barrier in atmosphere and surface ocean ENSO predictability, and therefore, it provides information about the irreversibility of the coupled ocean-atmosphere system.

A sudden increase or decrease in heat content can indeed occur at any time of the year, regardless of the phase of the ENSO oscillation. For example, *Hu and Fedorov* [2016] showed that a fast increase in heat content followed the January-to-March 2014 westerly wind bursts in the western Pacific, and a major decrease occurred immediately after the unusually strong basin-wide easterly wind burst in June 2014. These changes were relatively fast given that wind bursts generated Kelvin and Rossby waves that modified the depth of the thermocline as they were traveling along the zonal axis. This type of increase (decrease) in heat content is different from the meridional recharge (discharge) occurring during the mature phase of LN (EN). According to the recharge theory [*Jin*, 1997], the off-equatorial wind stress curl determines the tendency toward equatorward mass convergence (poleward mass divergence), and therefore the recharge (discharge) in tropical heat content through the meridional displacement of water masses. In this case, however, given that only the tendency is determined by winds, this process is relatively slower.

The present work highlights the asymmetry between the impact of a sudden increase or decrease in ocean heat content on subsequent EN events. We find that the timing and magnitude of the episodes are not substantially affected by the phase at which a sudden rise is prescribed: (1) TM + 80%: peak in year 0, Niño3.4 = +4°C; (2) RP + 80%: peak in year 0, Niño3.4 = +4°C.

In this regard, even if there are substantial differences in the mechanisms involved, EN events are seen to be independent from the timing of a sudden subsurface heat content reinforcement, given that the larger warming rate in the RP + 80% experiment quickly transforms the subsurface heat content into surface temperature anomalies. This result provides support to the hypothesis that the transition from the tilting mode to

the recharge phase is a necessary step for the onset of EN events [*Meinen and McPhaden*, 2000] and that it cannot be fastened or bypassed by suddenly increasing the heat content in the western Pacific or in the whole basin. In contrast, the timing and magnitude of EN episodes are substantially affected by the phase at which a large decrease in heat content is prescribed, given that the restoring process reinforcing the heat content and delaying the event by 1 year only takes place when heat is largely removed during the tilting mode: (1) TM-80%: peak in year 1, Niño3.4 = +2°C; (2) RP-80%: peak in year 0, Niño3.4 = +1.15°C. No such behavior is instead seen if the decrease occurs later during the recharge phase.

The asymmetry in the response to the increased and decreased heat content scenarios is explained by the direct relationship between the wind power (i.e., zonal wind stress acting on the kinetic energy of surface currents) and the buoyancy power (i.e., anomalous tilt of the equatorial thermocline sustained by the kinetic energy of the ocean currents [*Brown et al.*, 2011]). In the initially increased experiments, the additional heat is rapidly released regardless of the phase of the oscillation in which it is prescribed, because the unmodified trade winds cannot sustain the anomalous slope of the thermocline resulting from the superimposed heat content. Instead, in the initially decreased experiments, the unmodified winds can sustain and eventually reinforce the imposed more stable flatter slope of the thermocline. In this case, the response of the coupled ocean-atmosphere system indeed depends on the stage of the oscillation (i.e., state of the thermocline) in which the anomalous heat content is decreased.

Acknowledgments

J.B. gratefully acknowledges funding from the European Commission through a Marie Curie International Outgoing Fellowship (project MEMENTO from the FP7-PEOPLE-2011-IOF call) and a Marie Curie Individual Fellowship (project ACCLIM from the H2020-MSCA-IF-2016 call) and from the European Commission and the Catalan Government through a Marie Curie-Beatriu de Pinós Fellowship (project 00068 from the BP-DGR-2014-B call). All data sets used in this study are presented in this paper and in the supporting information file.

References

Ballester, J., M. A. Rodríguez-Arias, and X. Rodó (2011), A new extratropical tracer describing the role of the western Pacific in the onset of El Niño: Implications for ENSO understanding and forecasting, *J. Clim.*, *24*, 1425–1437.

Ballester, J., J. C. Burns, D. Cayan, Y. Nakamura, R. Uehara, and X. Rodó (2013), Kawasaki disease and ENSO-driven wind circulation, *Geophys. Res. Lett.*, *40*, 2284–2289, doi:10.1002/grl.50388.

Ballester, J., S. Bordoni, D. Petrova, and X. Rodó (2015), On the dynamical mechanisms explaining the western Pacific subsurface temperature buildup leading to ENSO events, *Geophys. Res. Lett.*, *42*, 2961–2967, doi:10.1002/2015GL063701.

Ballester, J., S. Bordoni, D. Petrova, and X. Rodó (2016a), Heat advection processes leading to El Niño events as depicted by an ensemble of ocean assimilation products, *J. Geophys. Res. Oceans*, *121*, 3710–3729, doi:10.1002/2016JC011718.

Ballester, J., R. Lowe, P. Diggle, and X. Rodó (2016b), Modelling and prediction of climate and health impacts: Challenges and opportunities, *Ann. N.Y. Acad. Sci.*, doi:10.1111/nyas.13129.

Ballester, J., D. Petrova, S. Bordoni, B. Cash, M. García-Díez, and X. Rodó (2016c), Sensitivity of El Niño intensity and timing to preceding subsurface heat magnitude, *Sci. Rep.*, *6* 36344.

Balmaseda, M. A., M. K. Davey, and D. L. T. Anderson (1995), Decadal and seasonal dependence of ENSO prediction skill, *J. Clim.*, *8*, 2705–2715.

Balmaseda, M. A., K. Mogensen, and A. T. Weaver (2013), Evaluation of the ECMWF ocean reanalysis system ORAS4, *Q. J. R. Meteorol. Soc.*, *139*, 1132–1161.

Barnston, A. G., M. K. Tippett, M. L. L'Heureux, S. Li, and D. G. DeWitt (2012), Skill of real-time seasonal ENSO model predictions during 2002–11: Is our capability increasing?, *Bull. Am. Meteorol. Soc.*, *93*, 631–651.

Bjerknes, J. (1969), Atmospheric teleconnections from the equatorial Pacific, *Mon. Weather Rev.*, *97*, 163–172.

Brown, J. N., A. V. Fedorov, and E. Guilyardi (2011), How well do coupled models replicate ocean energetics relevant to ENSO?, *Clim. Dyn.*, *36*, 2147–2158.

Chen, D., M. A. Cane, A. Kaplan, S. E. Zebiak, and D. Huang (2004), Predictability of El Niño over the past 148 years, *Nature*, *428*, 733–736.

Fedorov, A. V., S. Hu, M. Lengaigne, and E. Guilyardi (2015), The impact of westerly wind bursts and ocean initial state on the development, and diversity of El Niño events, *Clim. Dyn.*, *44*, 1381–1401.

Jin, F. F. (1997), An equatorial ocean recharge paradigm for ENSO. Part I: Conceptual model, *J. Atmos. Sci.*, *54*, 811–829, doi:10.1175/1520-0469(1997)054<0811:AEORPF>2.0.CO;2.

Hu, S., and A. V. Fedorov (2016), Exceptionally strong easterly wind burst stalling El Niño of 2014, *Proc. Nat. Acad. Sci. U.S.A.*, doi:10.1073/pnas.1514182113.

Hurrell, J. W., et al. (2013), The community earth system model: A framework for collaborative research, *Bull. Am. Meteorol. Soc.*, *94*, 1339–1360.

Izumo, T., J. Vialard, M. Lengaigne, M. C. de Boyer, S. K. Behera, J. J. Luo, S. Cravatte, S. Masson, and T. Yamagata (2010), Influence of the state of the Indian Ocean Dipole on the following year's El Niño, *Nat. Geosci.*, *3*, 168–172.

Kalnay, E., et al. (1996), The NCEP/NCAR 40-year reanalysis project, *Bull. Am. Meteorol. Soc.*, *77*, 437.

Kessler, W. S. (2002), Is ENSO a cycle or a series of events?, *Geophys. Res. Lett.*, *29*(23), 2125, doi:10.1029/2002GL015924.

McGregor, S., A. Timmermann, N. Shneider, M. Stuecker, and M. England (2012), The effect of the South Pacific convergence zone on the termination of El Niño events and the meridional asymmetry of ENSO, *J. Clim.*, *25*, 5566–5586.

McPhaden, M. J. (2003), Tropical Pacific Ocean heat content variations and ENSO persistence barriers. *Geophys. Res. Lett. 30*(9), 1480, doi:10.1029/2003GL016872.

McPhaden, M. J., S. E. Zebiak, and M. H. Glantz (2006), ENSO as an integrating concept in Earth Science, *Science*, *314*, 1740.

Meinen, C. S., and M. J. McPhaden (2000), Observations of warm water volume changes in the equatorial Pacific and their relationship to El Niño and La Niña, *J. Clim.*, *13*, 3551–3559.

Petrova, D., S. J. Koopman, J. Ballester, and X. Rodó (2016), Improving the long-lead predictability of El Niño using a novel forecasting scheme based on a dynamic components model, *Clim. Dyn.*, doi:10.1007/s00382-016-3139-y.

Picaut, J., F. Masia, and Y. du Penhoat (1997), An advective-reflective conceptual model for the oscillatory nature of ENSO, *Science*, *277*, 663–666.

Ramesh, N., and R. Murtugudde (2013), All flavours of El Niño have similar early subsurface origins, *Nat. Clim. Change*, *3*, 42–46.
Suarez, M. J., and P. S. Schopf (1988), A delayed action oscillator for ENSO, *J. Atmos. Sci.*, *45*, 3283–3287.
Wang, C., and J. Picaut (2004), Understanding ENSO physics—A review, in *Earth's Climate*, edited by C. Wang, S. P. Xie, and J. A. Carton, pp. 21–48, AGU, Washington, D. C.
Weisberg, R. H., and C. Wang (1997), A western Pacific oscillator paradigm for the El Niño–Southern Oscillation, *Geophys. Res. Lett.*, *24*, 779–782, doi:10.1029/97GL00689.
Wyrtki, K. (1985), Water displacements in the Pacific and the genesis of El Nino cycles, *J. Geophys. Res.*, *90*, 7129–7132, doi:10.1029/JC090iC04p07129.